

# Unsteady Waves Generated by Flow over a Porous Layer

L.H. Wiryanto

**Abstract**—A linear model of free surface flow is derived from two boundary value problems, each of which presents a flow in a different medium. The upper medium is fluid, and the lower one is porous medium. Since the flow is disturbed by an un-flat surface of the porous medium, the disturbance is then performed to the fluid surface as surface waves. The model is generalization of the impermeable bottom and also generalization of the steady flow. We solve the model numerically by a finite difference method of forward time averaged centered space. As a result, we perform the wave generation of the flow disturbed by bumps on porous layer. The effect of the uniform upstream and the porous layer is observed to the generated surface wave.

**Index Terms**—Permeable bed, Darcy's law, potential function, shifted phase.

## I. INTRODUCTION

A 2-D fluid flow is considered over permeable bed. We assume that the fluid is ideal and the flow is irrotational, so that the flow can be presented as a potential function. Far upstream the flow is uniform with velocity  $U_0$  and depth  $h_0$ . Since the surface of the bed is not flat, the flow is disturbed and it generates surface wave. The similar problem can be seen in Wiryanto [1] for a flow over an impermeable bed. He derived the model by series expansion and performed two solitary like waves, each of which travels in different direction as the transient waves for subcritical flow. In case the flow is supercritical, the waves tend to steady and confirm the result of steady free-surface flow by Vanden-Broeck [2].

Meanwhile, Mizumura [3] reported the work for steady flow over a wavy permeable bed. Series expansion was used to extract the first and second orders of the problem. A separation of variables was then applied to solve the problem. This method was also used by Wiryanto and Anwarus [4] for monochromatic-wave propagation over a permeable bed, and Wiryanto [5] for wave propagation passing a bump. As a result, there is a phase shift of the fluid surface, relative to the wavy bed form. We confirm the result through an unsteady model in this paper. For other works related to the phase shift can be seen such as Iwasa and Kennedy [6] who used the shear-flow theory. Ho and Gelhar in [7] and [8] studied the effects of the permeable wavy boundary in turbulent pipe flow using air. Mizumura [9] gave the detailed difference of the water surface profile in supercritical and subcritical flows using the potential flow theory.

In this paper we derive the model of unsteady flow over a permeable bed. The surface of the bed is not flat to disturb the flow, and it generates surface waves. We use the potential flow theory for the fluid medium and a linear

Darcy equation for the porous medium. For each medium, the potential function satisfies a boundary value problem of Laplace's equation, and they are approximated by assuming that the fluid is shallow, and the generated waves have long wavelength but small amplitude. Based on that assumption, the problem can be expressed as a couple of equations in variables of surface elevation and depth-average velocity. Many studies of flow in porous media use Darcy's law such as Liu and Wen [10]. They modeled the wave propagation in porous media into a diffusive equation. Similarly, Wiryanto and Djohan [11] developed the model in [10] for a system of two porous layers. The model can be considered as the simplification of surface wave propagation in mangrove forests, see Massel *et. al.* [12].

Our model is then solved numerically by a finite difference method to observe the effect of the parameters, i.e. Froude number  $F$  and Reynolds number  $R$  representing the uniform flow and the characteristic of the porous medium, and to observe the effect of surface bed profile to the generated waves. For some cases, we show that the model is able to explain the results in [1] and [3], as the limiting case either when the bed tends to impermeable or when the bed surface is made wavy.

## II. PROBLEM FORMULATION

The problem formulated here is illustrated in Figure 1. Far upstream a fluid flows uniformly with depth  $h_0$  and velocity  $U_0$ . The fluid lies above and occupies the pores of a permeable bed having permeability  $K$ . As the system of coordinates, we choose Cartesian with the horizontal  $\bar{x}$ -axis along the undisturbed level of the free surface, so that we can define the fluid elevation as  $\bar{y} = \bar{\eta}(\bar{x}, \bar{t})$ . The surface of the permeable bed is  $\bar{y} = -(h_0 + \bar{h}(\bar{x}))$ , and the solid bottom of the bed is flat with  $\bar{y} = -\bar{d}$ . Moreover, we use  $\bar{\phi}$  and  $\bar{\phi}'$  as the potential function in the fluid medium and in the porous medium.

Mathematically, the problem is to determine  $\bar{\phi}$ , and also  $\bar{\phi}'$ , satisfying

$$\bar{\phi}_{\bar{x}\bar{x}} + \bar{\phi}_{\bar{y}\bar{y}} = 0 \quad (1)$$

in the upper medium  $-(h_0 + \bar{h}(\bar{x})) < \bar{y} < \bar{\eta}(\bar{x}, \bar{t})$ . The kinematic and dynamic conditions on  $\bar{y} = \bar{\eta}$  are

$$\bar{\eta}_{\bar{t}} + \bar{\phi}_{\bar{x}}\bar{\eta}_{\bar{x}} - \bar{\phi}_{\bar{y}} = 0 \quad (2)$$

$$\bar{\phi}_{\bar{t}} + \frac{1}{2}(\bar{\phi}_{\bar{x}}^2 + \bar{\phi}_{\bar{y}}^2) + g\bar{\eta} = \frac{1}{2}U_0^2. \quad (3)$$

The right hand side of (3) is constant, obtained by comparing to the condition at the upstream, and  $g$  is gravitational acceleration.

Meanwhile, the conditions on the interface between the upper and lower media are expressed from the physical interpretation the continuity of the pressure and the mass

Manuscript received May 10th, 2010.

L.H. Wiryanto is with Faculty of Mathematics and Natural Sciences, Bandung Institute of Technology, Jalan Ganesha 10 Bandung- Indonesia, phone: +62 22 2502545, fax: +62 22 2506450, e-mail: leo@math.itb.ac.id

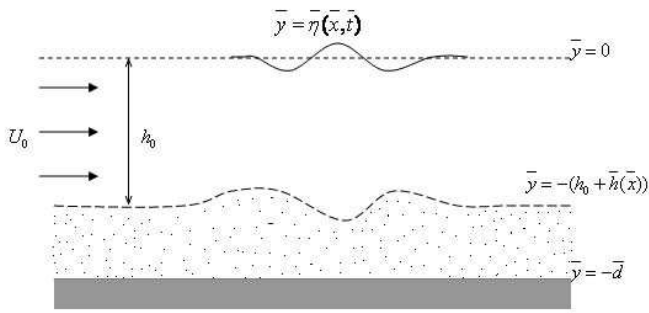


Fig. 1. Sketch of the flow over permeable bed

balancing of the fluid moving from one to other medium. The first condition is obtained by eliminating the pressure  $p$  from Bernoulli equation

$$\bar{\phi}_{\bar{t}} + \frac{1}{2} (\bar{\phi}_{\bar{x}}^2 + \bar{\phi}_{\bar{y}}^2) + g\bar{y} + \frac{p}{\rho} = \frac{1}{2} U_0^2 \quad (4)$$

for the upper medium and the pressure  $p'$  from Darcy's law in the lower medium following Mizumura [3], i.e.

$$\bar{\phi}' = -K(\rho g \bar{y} + p')/\nu \quad (5)$$

where  $\nu$  is viscosity and  $\rho$  is fluid density. Therefore, we have

$$\bar{\phi}_{\bar{t}} + \frac{1}{2} (\bar{\phi}_{\bar{x}}^2 + \bar{\phi}_{\bar{y}}^2) - \frac{\nu}{K\rho} \bar{\phi}' = \frac{1}{2} U_0^2 \quad (6)$$

along the interface.

The second condition on the interface is obtained by equating the total derivative of  $\bar{y} = -(h_0 + \bar{h}(\bar{x}))$  from both media, i.e.

$$\bar{\phi}_{\bar{x}} \bar{h}_{\bar{x}} + \bar{\phi}_{\bar{y}} = \bar{\phi}'_{\bar{x}} \bar{h}_{\bar{x}} + \bar{\phi}'_{\bar{y}}. \quad (7)$$

Consequently, the continuity equation is satisfied for both media, so that Laplace's equation of  $\bar{\phi}$  and  $\bar{\phi}'$  can be used such as given in (1) and also

$$\bar{\phi}'_{\bar{x}\bar{x}} + \bar{\phi}'_{\bar{y}\bar{y}} = 0. \quad (8)$$

Equation (8) is followed by the condition at the bottom of the porous medium  $\bar{y} = -d$ , i.e.

$$\bar{\phi}'_{\bar{y}} = 0. \quad (9)$$

In order to observe long waves on shallow water, we introduce the scaled variables, with respect to wavelength  $\lambda$ , fluid depth  $h_0$  and amplitude  $a$ , written by notations without bar as follows

$$\left. \begin{aligned} \bar{x} &= \lambda x, \quad \bar{y} = h_0 y, \quad \bar{t} = \frac{\lambda}{\sqrt{gh_0}} t, \quad \bar{\eta} = a \eta, \\ \bar{\phi} &= \frac{\lambda U_0 a}{h_0} \phi, \quad \bar{\phi}' = \frac{\lambda U_0 a}{h_0} \phi'. \end{aligned} \right\} \quad (10)$$

Moreover, we express the potential function  $\bar{\phi}$  as

$$\bar{\phi} = U_0 \bar{x} + \bar{\Phi} \Leftrightarrow \phi = \frac{h_0}{a} x + \Phi \quad (11)$$

representing the uniform stream and its perturbation. Therefore, the governing equations (1) and (8) become

$$\mu^2 \Phi_{xx} + \Phi_{yy} = 0, \quad (12)$$

$$\mu^2 \phi'_{xx} + \phi'_{yy} = 0. \quad (13)$$

The boundary conditions (2) and (3) along the surface  $y = \epsilon \eta(x, t)$  become

$$\mu^2 \eta_t + F \mu^2 \eta_x + F \epsilon \mu^2 \Phi_x \eta_x - F \Phi_y = 0, \quad (14)$$

$$F \Phi_t + \frac{1}{2} F^2 \left( 2 \Phi_x + \epsilon \Phi_x^2 + \frac{\epsilon}{\mu^2} \Phi_y^2 \right) + \eta = 0. \quad (15)$$

The conditions (6) and (7) along the interface  $y = -(1 + \epsilon h(x))$  become

$$\Phi_t + F \Phi_x + \frac{1}{2} F \epsilon \Phi_x^2 + \frac{1}{2} \frac{\epsilon}{\mu^2} \Phi_y^2 - \frac{F}{R} \phi' = 0 \quad (16)$$

$$\mu^2 h_x + \mu^2 \epsilon \Phi_x h_x + \Phi_y = \mu^2 \epsilon \phi'_x h_x + \phi'_y; \quad (17)$$

and the condition on the bottom  $y = -d$  is

$$\phi'_y = 0. \quad (18)$$

$\epsilon$  and  $\mu$  are two small parameters defined by

$$\epsilon = \frac{a}{h_0}, \quad \mu = \frac{h_0}{\lambda},$$

and we denote non-dimensional quantities

$$d = \frac{\bar{d}}{h_0}, \quad h(x) = \bar{h}(\bar{x}),$$

the Froude number  $F = U_0/\sqrt{gh_0}$  and Reynolds number  $R = U_0 \rho K / (\nu \lambda)$ .

The potential functions  $\Phi$  and  $\phi'$  are then determined from the governing equations (12) with condition (14); and (13) with condition (18). When we substitute

$$\left. \begin{aligned} \Phi &= \Phi_0 + \epsilon \Phi_1 + \epsilon^2 \Phi_2 + \dots \\ \phi' &= \phi'^{(0)} + \epsilon \phi'^{(1)} + \epsilon^2 \phi'^{(2)} + \dots \end{aligned} \right\} \quad (19)$$

to those equations and using  $\epsilon = \mu^2$ , the system of equations can be analyzed order by order, giving

$$\left. \begin{aligned} \Phi &= \Phi_0(x, t) + \epsilon \left( -\frac{1}{2} \Phi_{0xx} y^2 + \left( \frac{1}{F} \eta_t + \eta_x \right) y + \Phi_{10}(x, t) \right) + \dots \\ \phi' &= \phi'^{(0)}(x, t) + \epsilon \left( -\frac{1}{2} \phi'^{(0)}_{xx} (y+d)^2 + \phi'^{(10)}(x, t) \right) + \dots \end{aligned} \right\} \quad (20)$$

where  $\Phi_0, \Phi_{10}, \phi'^{(0)}$  and  $\phi'^{(10)}$  are unknown function of  $x$  and  $t$ . The potential functions (20) are then substituted into (15), (16) and (17); the leading order is

$$\left. \begin{aligned} F \Phi_{0t} + F^2 \Phi_{0x} + \eta &= 0 \\ h_x + \Phi_{0xx} + \frac{1}{F} \eta_t + \eta_x &= \phi'^{(0)}_{xx} (1-d) \\ \Phi_{0t} + F \Phi_{0x} - \frac{F}{R} \phi'^{(0)} &= 0. \end{aligned} \right\} \quad (21)$$

We can reduce the result (21) into two equations by eliminating  $\phi'^{(0)}$ . This is then followed by defining the depth-average velocity

$$u = \frac{1}{1 + \epsilon \eta + \epsilon h} \int_{-1-\epsilon h}^{\epsilon \eta} \Phi_x dy \quad (22)$$

and using (20) to (22), so that we have  $u \approx \Phi_{0x}$ . Therefore, (21) becomes

$$\left. \begin{aligned} F u_t + F^2 u_x + \eta_x &= 0 \\ \eta_t + F(\eta_x + u_x + h_x) &= (1-d)R(u_{xt} + F u_{xx}) \end{aligned} \right\} \quad (23)$$

as the model. The effect of the permeable bed can be seen as the right hand side of the second equation of (23). The ability of the bed to absorb the fluid is presented by  $R$  and  $d$ , but they cannot be observed separately since they appear as one coefficient. The model without porous medium can be obtained by setting  $R = 0$ , and this model agrees to the linear equations in Wiryanto [4].

III. NUMERICAL PROCEDURE

From the derivation in the previous section, the problem is to determine  $\eta$  and  $u$  in the model (23). We solve the model numerically by a finite difference method of forward-time average centered-space, described in this section. We first discretize the space  $x$  and time  $t$  domains by defining  $x = j\Delta x$  for  $j = 0, 1, 3, \dots, J$  and  $t = n\Delta t$  for  $n = 0, 1, 2, \dots$ ; so that we approximate  $\eta$  and  $u$  by denoting

$$\eta(x, t) \approx \eta_j^n, \quad u(x, t) \approx u_j^n. \quad (24)$$

Before discretizing (23), we replace  $u_{xt} + Fu_{xx}$  in the second equation using the first equation, so that the second equation of (23) becomes

$$\eta_t + F(\eta_x + u_x + h_x) = \frac{(d-1)R}{F}\eta_{xx}. \quad (25)$$

Now the difference equations are

$$F \frac{u_j^{n+1} - u_j^n}{\Delta t} + F^2 \frac{u_{j+1}^{n+1} - u_{j-1}^{n+1} + u_{j+1}^n - u_{j-1}^n}{4\Delta x} + \frac{\eta_{j+1}^{n+1} - \eta_{j-1}^{n+1} + \eta_{j+1}^n - \eta_{j-1}^n}{4\Delta x} = 0 \quad (26)$$

and

$$\frac{\eta_j^{n+1} - \eta_j^n}{\Delta t} + F \left( \frac{\eta_{j+1}^{n+1} - \eta_{j-1}^{n+1} + \eta_{j+1}^n - \eta_{j-1}^n}{4\Delta x} + \frac{u_{j+1}^{n+1} - u_{j-1}^{n+1} + u_{j+1}^n - u_{j-1}^n}{4\Delta x} + h_x \right) = A \left[ \frac{\eta_{j+1}^{n+1} - 2\eta_j^{n+1} + \eta_{j-1}^{n+1} + \eta_{j+1}^n - 2\eta_j^n + \eta_{j-1}^n}{2\Delta x^2} \right] \quad (27)$$

where  $A = (d-1)R/F$ . Note that  $h_x$  is approximated by

$$h_x \approx \frac{h_{j+1} - h_{j-1}}{2\Delta x}$$

from a given surface profile of the bed.

Since both (26) and (27) contain  $u$  and  $\eta$  at the time step  $n + 1$ , we need a predictor of  $\eta_j^{n+1}$  to calculate  $u_j^{n+1}$  in (26), and then  $\eta$  is corrected by (27) using  $u_j^{n+1}$  from previous calculation. The predictor of  $\eta$  is evaluated from (25) discretized into

$$\frac{\eta_j^{n+1} - \eta_j^n}{\Delta t} + F \left( \frac{\eta_{j+1}^n - \eta_{j-1}^n}{2\Delta x} + \frac{u_{j+1}^n - u_{j-1}^n}{2\Delta x} \right) + Fh_x = A \left[ \frac{\eta_{j+1}^n - 2\eta_j^n + \eta_{j-1}^n}{\Delta x^2} \right] \quad (28)$$

In solving the model corresponding to (26) and (27), we apply Gauss-Seidel iteration for the system of linear equations constructed from each equation. The system is a closed form by involving left and right values of  $\eta$  and  $u$  outside of the domain. In this case we use  $\eta_{-1}^n = 0, u_{-1}^n = 0$  presenting the left boundary that is relatively far from disturbance and still uniform. Since  $\eta_{j+1}^n$  and  $u_{j+1}^n$  are required in calculation in the next time step, we can extrapolate them linearly. Physically, this is condition for wave absorption. Therefore, the calculation has to be stopped when the wave approaches the left boundary. As the initial condition, we translate from the physical situation, at the beginning the fluid surface and the velocity are undisturbed from uniform flow, so that we use  $\eta_j^0 = 0, u_j^0 = 0$ .

IV. NUMERICAL RESULTS

The numerical scheme described above is used to calculate the elevation  $\eta$  and velocity  $u$  for various values of parameters  $F, R, d$ ; and  $h(x)$  the surface of the permeable bed. Since the parameters  $d$  and  $R$  appear as one coefficient of  $\eta_{xx}$  in (25), the effect of both parameters is then observed as  $R(d-1)$ . Most calculations here use  $\Delta x = 0.1$  and  $\Delta t = 0.02$ . Our calculations are stopped when the generated waves relatively close to the left boundary. Most of them is calculated up to  $t = 48$  or  $n = 2400$ . At that time, the fluid surface is relatively steady. When we plot the amplitude with respect to the time  $t$ , it gives an asymptotical curve.

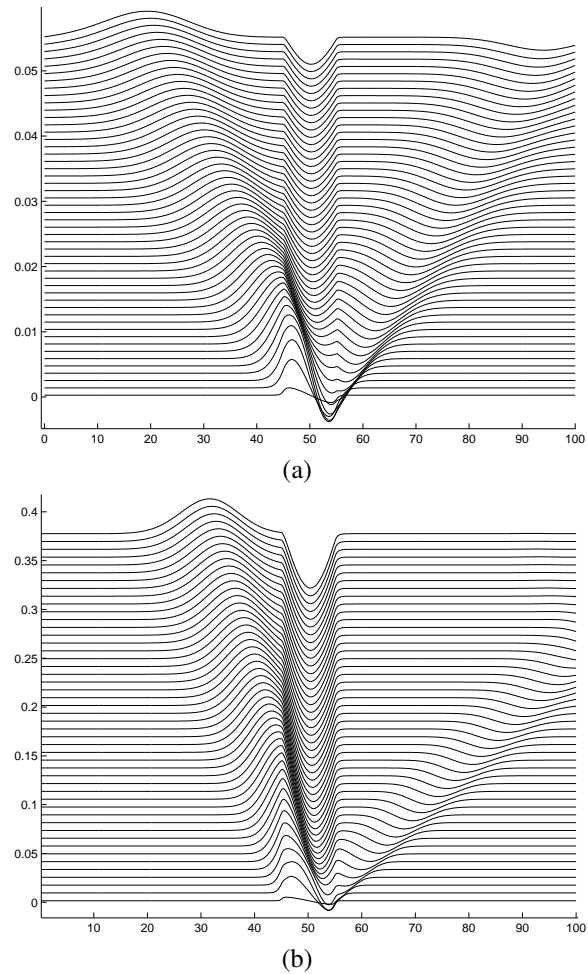


Fig. 2. Waves generated by flow over a permeable bed for (a)  $F = 0.2, R(d-1) = 0.3$ ; and (b)  $F = 0.6, R(d-1) = 0.3$ .

First, we consider for the surface of the permeable bed in form of a sinusoidal bump

$$h(x) = -0.1 \sin(\pi(x - 45)/10)$$

located at  $x \in [45, 55]$ . Note that the interface between the upper and lower (porous) media is  $y = -(1 + \epsilon h(x))$ . The negative sign in  $h$  indicates that the bump is above  $y = -1$ . The incoming flow is disturbed by the bump, and it generates surface waves. In Figure 2, we plot the elevation  $\eta$  for different values of  $t$  in the same plane, but shifted upward for larger  $t$ . Mainly, the flow generates waves, going to the left, right and remain above the bump. The wave generation shown in Fig. 2 (a) calculated using  $F = 0.2, R(d-1) = 0.3$  as typical wave propagation for small Froude number. Plot

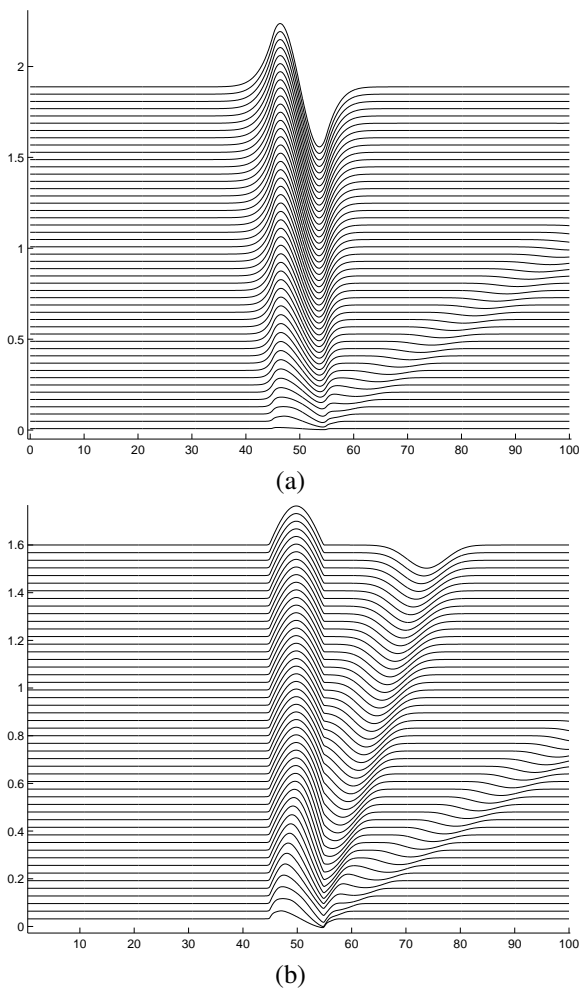


Fig. 3. Waves generated by flow over a permeable bed for (a)  $F = 1.0$  and (b)  $F = 1.6$ ;  $R(d-1) = 0.3$ .

in Fig. 2 (a) can be compared to waves for larger Froude number shown in Fig. 2 (b), corresponding to  $F = 0.6$  and the same value  $R(d-1)$ . We obtain that the waves have larger amplitude for larger  $F$ . This is followed by smaller speed for the left going wave. We can see from the characteristic line, i.e. a line connecting the maximum point on the surface at any time. The tangential of the line is more vertical for larger  $F$ . On the other hand, the speed of the right going wave increases by increasing  $F$ . When we continue by increasing  $F$ , we have no left going wave. The flow with  $F = 1$  is the critical situation where the left going wave has zero wave speed, i.e. the wave remains above the bump, as shown in Figure 3 (a). As the comparison we show the wave generation for supercritical flow with two waves traveling to the right in Figure 3 (b). The surface above the bump has the same profile to the interface. For subcritical flow  $F < 1$ , we have different concave between surface and interface.

Now, we observe the left going wave resulted by flow of  $F = 0.2$ . We measure the amplitude of the wave and the maximum of the particle velocity  $u$  for each time step. We obtain that the wave grows up and then decreases the amplitude with dissipating the wave energy. The particle velocity  $u$  corresponding to the wave is negative, but much smaller than the uniform velocity, and it tends to zero as  $t \rightarrow \infty$ . Therefore, the left going wave will disappear for long run. Similar result is also obtained for right going wave, with

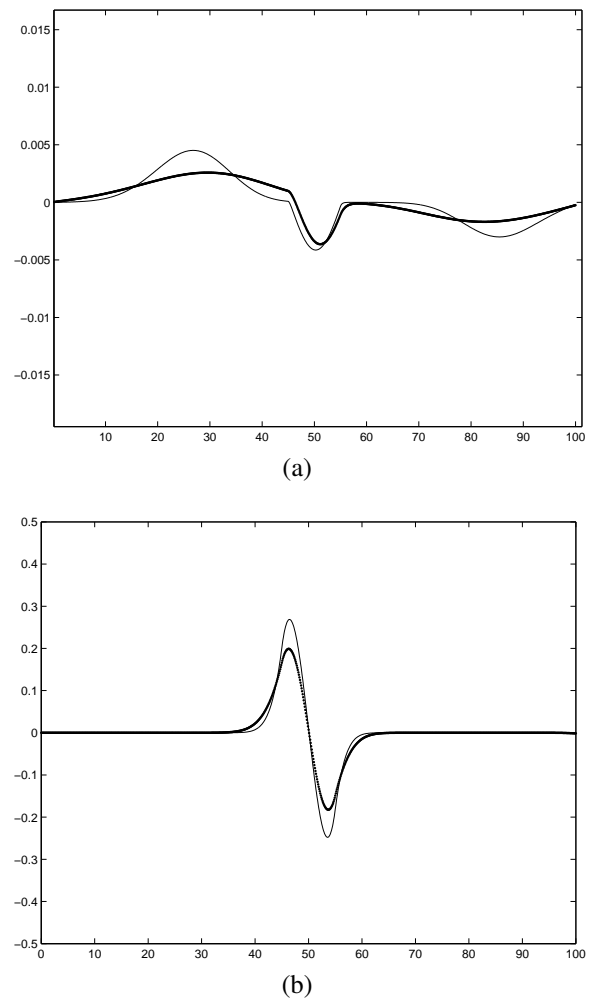


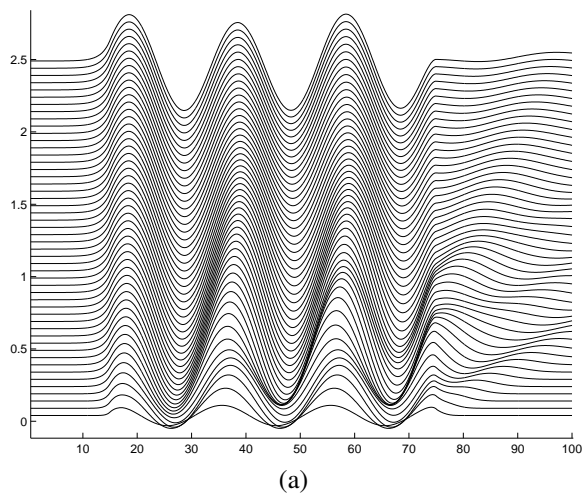
Fig. 4. Plot of  $\eta(x, 30)$  for  $R(d-1) = 0.3$  and  $1.0$ , using (a)  $F = 0.2$  and (b)  $F = 1.0$ .

negative surface elevation. Meanwhile, the surface profile above the bump has amplitude asymptotically to a certain value, so that this profile is as the steady solution. For other values  $F$  we obtain similar result, the left and right going waves will disappear, and the steady solution is concave up or down depending on the flow, subcritical or supercritical.

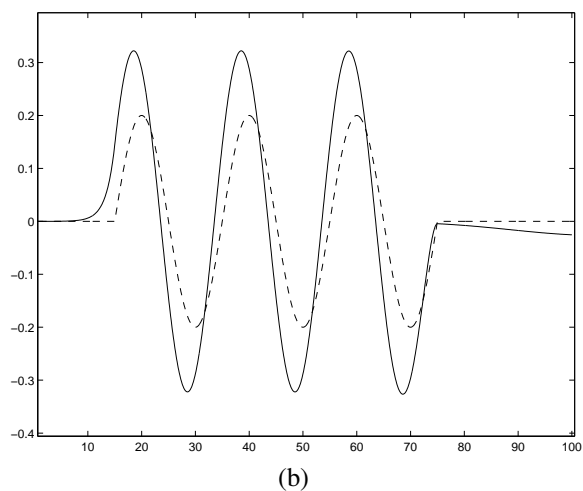
The effect of the porous layer is then observed by considering the amplitude and the deformation of the waves for different values  $R(d-1)$ . Our model can explain the dissipation of the wave energy generated by flow as described above. The quantity related to the porous layer appears in diffusion term of  $\eta_{xx}$ , damping the waves. Therefore, the numerical solution performs waves having amplitude asymptotical to smaller value for larger  $R(d-1)$ , and the damping of the waves is stronger as the diffusion term contributes stronger. We show in Figure 4 (a) plot of  $\eta(x, 30)$  corresponding to  $R(d-1) = 0.3$  and  $1$  (bold line), for  $F = 0.2$ . In Figure 4 (b) we show the result for  $F = 1.0$ . When the lower layer is solid, i.e.  $R = 0$ , the waves are generated by the flow and travel solitary like waves as obtained in Wiryanto [1], and the steady solution confirms to the result in Vanden Broeck [2] for supercritical flow.

Now we consider for the surface of the permeable bed by setting

$$h(x) = -0.2 \sin(\pi(x - 15)/10)$$



(a)



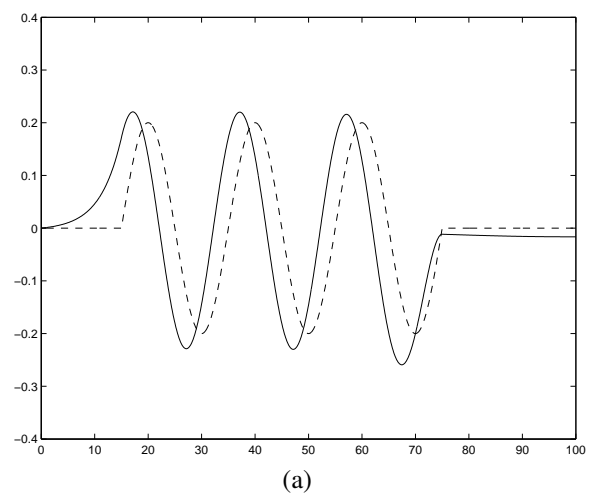
(b)

Fig. 5. (a) Wave generation by flow over permeable wavy bed, (b) the steady waves plotted together with the interface profile of the wavy bed (dash lines).

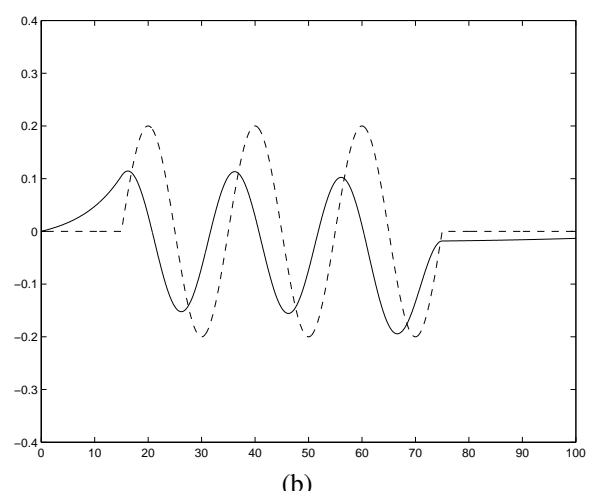
at  $x \in [15, 75]$ . Here we add the number of the bump to make comparison between the bed surface and the profile of the steady waves, also we choose supercritical flow ( $F > 1$ ) to produce right-going waves, so that we can calculate for longer time. The propagation of the waves is shown in Figure 5 (a), calculated using  $F = 1.5$ ,  $R(d-1) = 2.0$ . If the calculation is continued for longer  $t$ , the elevation  $\eta$  is plotted together with the bed surface  $-h$ , given in dash line (-), in the same plane, shown in Figure 5 (b). We obtain that the surface elevation is shifted, namely  $\alpha$ , from the bed surface. For larger  $R(d-1)$  we obtain higher value of  $\alpha$ . As the comparison, we show in Figure 6 (a) corresponding to  $F = 1.5$ ,  $R(d-1) = 5$ , and Fig. 6 (b) for  $R(d-1) = 10$ . This agrees to Mizumura [3] who obtained the shifted phase analytically, directly from steady formulation. We can also compare the amplitude of the steady waves, that is smaller for larger  $R(d-1)$  as explain previously.

## V. CONCLUSIONS

A linear unsteady model has been derived for surface waves generated by flow passing a permeable wavy bed. The numerical scheme was formulated by a finite difference method based on forwarded time average centered space, and the solution was used to observe the deformation and



(a)



(b)

Fig. 6. The steady waves (solid curve) plotted together with the interface profile (dash lines) of the wavy bed for (a)  $R(d-1) = 5$ , and (b)  $R(d-1) = 10$ .

propagation of the fluid surface waves. Our numerical observation show that the wave generation is effected by the Froude number and the characteristic of the porous medium. The waves are absorbed partly by existing the permeable bed on the bottom of the channel. The steady waves are indicated to be obtained for long run, and the wave profile is shifted from the permeable surface, agrees to the results obtained by other researchers. Therefore, the model is able to explain the physical phenomena generalized from impermeable bottom and the case of steady flow.

## ACKNOWLEDGMENT

The Author is grateful to Indonesian Government for financial support through research grant, under project DP2M DIKTI no. 164/SP2H/PP/DP2M/V/2009, Research grants: 258/K01.7/PL/2009 and 249/K01.7/PL/2010. The Author also would like to thank to Dr. S.R. Pudjaprasetya, B. Supriyanto and P. Deffinika for stimulating discussion and correction of this paper.

## REFERENCES

- [1] L.H. Wiryanto, "A solitary-like wave generated by flow passing a bump," Submitted to *Proc. Int. Conf. Math. Stat. Its Appl.*, 2010.
- [2] J.-M. Vanden-Broeck, "Free-surface flow over an obstruction in a channel," *Phys. Fluids*, V30, N8, pp. 2315-2317, 1987.

- [3] K. Mizumura, "Free surface flow over permeable wavy bed," *J. Hydr. Engrg.*, V124, N9, pp. 955-962, 1998.
- [4] L.H. Wiryanto and Anwarus S., "Monochromatic waves over permeable bed," *Proc. 5th Asian Math. Conf. 2009*, pp. 617-622, 2009.
- [5] L.H. Wiryanto, "Wave propagation over a submerged bar," *ITB J. Sci.*, V42A(2), pp. 81-90, 2010.
- [6] Y. Iwasa and J.F. Kennedy, "Free surface shear flow over a wavy bed," *J. Hydr. Div.*, V94, N3, pp. 431-454, 1963.
- [7] R.T. Ho and L.W. Gelhar, "Turbulent flow with wavy permeable boundaries," *J. Fluid Mech.*, V58, N2, pp. 403-414, 1973.
- [8] R.T. Ho and L.W. Gelhar, "Turbulent flow over undular permeable boundaries," *J. Hydr. Engrg.*, V109, N5, pp. 741-756, 1983.
- [9] K. Mizumura, "Free surface profile of open channel flow with wavy boundary," *J. Hydr. Engrg.*, V121, N7, pp. 533-539, 1995.
- [10] P.L.-F. Liu and J. Wen, "Nonlinear diffusive surface waves in porous media," *J. Fluid Mech.*, V347, pp. 119-139, 1997.
- [11] L.H. Wiryanto and W. Djohan, "A mathematical model of surface waves in a system of two porous layers," *Int. J. Applied Math. Stat.*, V17, pp. 116-124, 2010.
- [12] S.R. Massel, K. Furukawa and R.M. Brinkman, "Surface wave propagation in mangrove forests," *Fluid Dyn. Research*, V24, pp. 219-249, 1999.